International Journal of Mathematical, Engineering and Management Sciences
Vol. 7, No. 4, 433-454, 2022
https://doi.org/10.33889/IJMEMS.2022.7.4.029

A Multi Objective Evolutionary Algorithm based on Decomposition for a Flow Shop Scheduling Problem in the Context of Industry 4.0

Diego Gabriel Rossit
Department of Engineering and INMABB,
Universidad Nacional del Sur and CONICET, Bahía Blanca, Buenos Aires, Argentina.
E-mail: diego.rossit@uns.edu.ar

Sergio Nesmachnow
Universidad de la República, Uruguay.
E-mail: sergion@fing.edu.uy

Daniel Alejandro Rossit
Department of Engineering and INMABB,
Universidad Nacional del Sur and CONICET, Bahía Blanca, Buenos Aires, Argentina.
Corresponding author: daniel.rossit@uns.edu.ar

(Received on April 03, 2022; Accepted on June 16, 2022)

Abstract
Under the novel paradigm of Industry 4.0, missing operations have arisen as a result of the increasingly customization of the industrial products in which customers have an extended control over the characteristics of the final products. As a result, this has completely modified the scheduling and planning management of jobs in modern factories. As a contribution in this area, this article presents a multi objective evolutionary approach based on decomposition for efficiently addressing the multi objective flow shop problem with missing operations, a relevant problem in modern industry. Tests performed over a representative set of instances show the competitiveness of the proposed approach when compared with other baseline metaheuristics.

Keywords- Industry 4.0, Flow shop, Missing operation, Evolutionary algorithms, Multi objective optimization, Makespan, Total tardiness.

1. Introduction
In recent years, digital tools have strongly penetrated production systems and their supply chains. From this, the possibility of managing the information associated with production processes has improved remarkably (Xu et al., 2018). The main technologies underlying these transformations are cyber-physical systems (CPS) and the Internet of Things (IoT). CPS allow the integration of physical production systems with all production planning functions (usually associated with digital technologies) into only one system. Thus, production orders are executed with greater precision, generating a more flexible production system. While IoT provides the means for all these interactions to take place. This new paradigm is called Industry 4.0 (Lee et al., 2015).

Information Technologies enhancement of production processes allows for a more fluid management of a broader portfolio of products, and to dispense of the rigid standardization that governs mass production models (Wang et al., 2017). In mass production environments, computer systems used to be rudimentary, and then, they were limited to manage information (needs for materials, operation routes, etc.) for a few products. However, by having current information tools and technologies, where the possibility of managing different sources of information is incorporated, personalized production models are gaining ground. These models allow customers to incorporate their specifications and preferences in their production orders, so that the resulting products are not all the same, but are adapted to the customer. Industry 4.0 has greatly enhanced these personalized production business strategies (Perez et al., 2022). However, personalized production challenges the decision-making processes for production planning, and particularly scheduling, because personalized orders dismiss the standardized production routes and incorporate new features. Then, scheduling problems become more difficult than they used to be. A clear example is flow shop scheduling problems with missing operations (Rossit et al., 2021a). Where, in the classic version of flow shop scheduling problem, all jobs have the same processing route, meanwhile in missing operation flow shop, some jobs may require or not some of the operations, which increases scheduling decision process.

In this article, a missing operation flow shop scheduling problem is addressed. The studied problem is a multi objective version of the flow shop problem with missing operations, considering the simultaneous optimization of makespan and total tardiness objectives. Makespan is a relevant metric since it describes the capacity utilization, and how the investment made in production lines is used. It measures the efficiency for the company, the lower the makespan for a given set of jobs, the better the capacity usage. In turn, total tardiness evaluates how the customer service is being achieved. For this, the delivery date of the customer order from the production system, is contrasted with the due date that was defined in agreement with the customer before the releasing of the order, and if it is computed only if there is delay. Obviously, the larger the delay, the poorer the performance (Pinedo, 2012). This problem is NP-hard in its single objective version (Lenstra et al., 1977), then the multi objective version is also NP-hard (Minella et al., 2008). Thus, for having an efficient approach for this problem a meta-heuristic algorithm is proposed.

Meta-heuristic algorithms have shown great capacity in handling multi objective scheduling problems (Yenisey and Yagmahan, 2014; Uniyal et al., 2020). In the case of this article, the proposed resolution approach applies the Multi Objective Evolutionary Algorithm based on Decomposition (MOEA/D), an evolutionary computation method that has been recognized as a promising tool for solving multi objective optimization problems by applying a divide-and-conquer approach (Zhang and Li, 2007). MOEA/D has shown great capability on solving flow shop scheduling problems (Chang et al., 2008) (Alhindi and Zhang, 2014; Wang et al., 2021). For this particular application, the proposed hybrid algorithm is based on a custom made version of the jmetal optimization framework, including specific modifications for leveraging its optimization capacities. These modifications are based on the normalization of the considered objective functions, which improve the scalar mono-objective optimization processes, and also a re-definition of the reference points for computing multi objective optimization metrics, which impacts on the solution assessments.

The main results of the reported research indicate that the proposed MOEA/Ds are competitive to address this combinatorial optimization problem since they were able to efficiently solve a representative set of instances with different percentages of missing operations. Moreover, the MOEA/Ds showed to be competitive when compared with other state-of-art metaheuristics used as baseline, obtaining better distributed Pareto fronts.

The article is organized as follows. Next section presents the main concepts about multi objective optimization and describes the multi objective version of the flow shop problem with missing operations. Section 3 outlines the resolution approach and describes the multi objective algorithm applied to solve the problem. The experimental evaluation of the proposed resolution approach is described in Section 4, which also reports and analyzes the experimental results. Finally, the conclusions of the research and the main lines for future work are formulated in Section 5.

2. Multi Objective Flow Shop Problem

This section presents the multi objective flow shop problem addressed in this article. The first subsection introduces the basic concepts of multi objective optimization problems and the main ideas of the optimization approach applied in this article. After that, the next subsection describes the scheduling problem addressed, i.e., multi objective flow shop with missing operations, and comments on the main contributions of the literature related to the problem.

2.1 Problem Description

This subsection describes the problem addressed at this work. For this, firstly, the main concepts about multi objective optimization problems are detailed, and then, the main features of the special flow shop case that is approached here.

2.1.1 Multi Objective Optimization Problems

Multi objective optimization problems arise when considering typical decision-making situations in real environments, such as those addressed in production planning, where issues of internal efficiency of the company must be addressed (e.g., minimizing costs or use of machines) simultaneously with issues related to the level of service for customers (e.g., measurement of compliance with the delivery date). This type of situation involves decisions with interests that are not directly comparable, and even many times, achieving optimal solutions in one of the interests is detrimental to the other interest. These types of problems require comparison strategies based on Pareto Dominance, where the solution vector x is analyzed in terms of s different objective functions $f_1(x), \ldots, f_s(x)$ simultaneously (Coello et al., 2007). To introduce these comparison criteria, we first present an illustrative description of the problem, which consists of a minimization problem, then, a multi objective problem can be defined by Equations 1-3, where p and q are the equations and inequalities that define the feasible set X, meaning that a solution x is valid only if $x \in X$. In the objective function (1), there are s objective functions, with $s \geq 2$. Thus, for comparing two solutions x_1 and x_2, such that $\{x_1, x_2\} \in X$, it is necessary to consider the Pareto Dominance criterion, which is accomplished by conditions (4) and (5).

$$\text{Min } \{f_1(x), \ldots, f_s(x)\}. \tag{1}$$

subject to

$$h_i(x) = 0, i = 1,2, \ldots, p \tag{2}$$
$$g_l(x) \leq 0, l = 1,2, \ldots, q \tag{3}$$
$$f_r(x_1) \leq f_r(x_2), r = 1,2, \ldots, s, \tag{4}$$
$$\exists r \in \{1,2, \ldots, s\}: f_r(x_1) < f_r(x_2). \tag{5}$$

and, the set of solutions x that accomplish conditions (4) and (5) is defined as the Pareto Optimal Front (POF).

2.2 Flow Shop Problem with Missing Operations

The flow shop problem is one of the most widely studied problems in the class of scheduling problems. The flow shop problem consists of sequencing a set N with n jobs, in a set M with m machines. Each job j ($j \in N$), consists of a set O_{ij} of operations; the i-th operation must be performed on machine i. The goal is to obtain a sequencing σ optimizing some criterion $f(\sigma)$. However, in this case, multiobjective problems will be studied, so the criteria to be optimized follow the structure presented in Equations (1-5), which is why the problem is especially difficult.

In turn, the studied problem has the peculiarity that not all jobs have the same number of operations, that is, some jobs do not need to be processed by all machines. That is to say that $|O_{ij}| \neq |O_{ij'}|, j \neq j'$. This situation occurs particularly in environments in which production tends to be personalized and the design of the product varies in small characteristics according to the client. This type of problem has taken a renewed interest since the advent of the fourth industrial revolution where the possibility of offering personalized products has been greatly increased.

However, within the first articles that have addressed this problem, Glass et al. (1999) addressed a two machine flow shop problem with no-wait conditions. The authors developed some heuristics that handle the problem in a sequential procedure, firstly they sequence the jobs that have an operation in each machine, and finally they insert the jobs with missing operations. Then, in (Rajendran and Ziegler, 2001) some dispatching rules are developed for minimizing the Total Flow Time, and in (Holthaus and Rajendra, 2002) similar dispatching rules are used for optimizing a dynamic buffer-constrained flow shop problem. In (Marichelvam and Prabaharan, 2014) a case study on a steel furniture manufacturing company is addressed, and for optimizing the problem a hybrid genetic scatter search algorithm is proposed. Traditional algorithms like Simulated Annealing, have shown to be capable of handling this complex problem (Venkataramanaiah, 2008, Rossit et al., 2021a). Venkataramanaiah (2008) addressed a cellular manufacturing problem considering the makespan, total flow time and idle time, applying a mono-objective approach using a weighted sum function. Meanwhile, Rossit et al. (2021a) considered an Industry 4.0 Cellular manufacturing environment, optimizing the Total Tardiness as the objective function.

Later, non-permutation solutions were considered for this problem. Pugazhendhi et al. (2003, 2004a, 2004b) studied a flow-line problem and designed new heuristics for optimizing the Total Flow Time, in the first two cases, and total weighted flow time and makespan in the latter one. The heuristics proposed are based on insertion procedures that enables creating non-permutation solutions, that is, the machines process the jobs in different orders. Tseng et al. (2008) highlighted the need of representing missing operations in scheduling problems, to represent more realistic situations. The authors developed non-permutation heuristics for a two stage hybrid flow shop problem. Henneberg and Neufeld (2016) designed and implemented a constructive heuristic and a Simulated Annealing algorithm to optimize the flow time. These optimization procedures include non-permutation solutions. Ramezanian and Rahmani (2017) developed a Mixed Integer Linear Programming (MILP) mathematical formulation for the problem where the makespan is the objective function and non-permutation solutions are considered. The MILP model was able to solve small-size instances, meanwhile for the large-size instances a genetic algorithm was developed. More recently, Dios et al. (2018) developed an extensive study on heuristics for coping with hybrid flow shop with missing operations, optimizing the makespan for over 50 different heuristics. Shao et al. (2020) and Shao et al. (2021) extended the scope of missing operations problems considering distributed hybrid flow shop problems. In the first case, the author developed iterated greedy algorithms for a distributed hybrid problem, meanwhile in the latter case, the same authors designed and proposed several constructive heuristics. In both articles the makespan is considered as objective function.

3. Resolution Approach: Multi Objective Evolutionary Algorithm based on Decomposition

There are different ways to address multi objective combinatorial optimization problems, such as exact approaches based in mathematical programming (Rossit et al., 2020) or heuristic and metaheuristic approaches (Toutouh et al., 2020). In complex combinatorial problems, as the one described in this paper, metaheuristics are suitable methods to obtain high-quality approximate solutions. Metaheuristics can obtain near-optimal solutions for NP-hard problems in very shorter computing times than exact methods (Rossit et al., 2021d). Moreover, they can address large realistic problem instances that are difficult to solve with exact methods due to long execution times.

This article considers a state-of-the-art multi objective evolutionary algorithm (MOEA) for addressing the target problem. Unlike the first single-objective genetic algorithms, the MOEAs were designed to solve problems in which there are two or more conflicting goals. These algorithms have been successfully applied in many real-world applications (Nesmachnow, 2014). Differently to other traditional multi objective resolution approaches that work with a weighted function that summarizes all the optimization criteria, MOEAs are population-based methods that can find a set of numerous solutions in a single execution. MOEAs were mainly devised to pursue two goals at the same time: to approximate the Pareto front of the optimization problem with its Pareto-based evolutionary search, and to maintain diversity of the solutions -instead of converging to a particular section of the Pareto front- through the use of diversification tools (e.g., sharing, crowding). Among the different MOEAs, this article applies a Multi objective Evolutionary Algorithm based on Decomposition (MOEA/D). MOEA/D is a well-known evolutionary algorithm that has proven to be relatively efficient in comparison with hypervolume-based and Pareto dominance-based algorithms in terms of their search ability and computation time (Zhang and Li, 2007) and has been successfully and extensively applied in many different application areas. This algorithm proposes a structured approach, generating a decomposition of the solution space in order to ensure broad coverage from the beginning (i.e., diversity). Then, to each region, product of the decomposition, it assigns a scalar vector and analyzes the dominance according to these scalar vectors (pursuing convergence). The general framework of MOEA/D is presented in Algorithm 1.

Algorithm 1: The MOEA/D general framework

INPUT: the number of the sub-problems considered in MOEA/D, N
a uniform spread of N weight vectors: $w^0, \ldots, w^N$
the number of the weight vectors in the neighborhood of each weight vector, T
the maximum number of generations, gen_{max}
OUTPUT: the set of non-dominated solutions (NS)

Step 0 - Setup:
NS $\leftarrow \emptyset$
$gen \leftarrow 0$
Step 1 - Initialization:
Uniformly randomly generate an initial population, $P(0)=\{x^0, \ldots, x^N\}$ and set the vector of values of the objective functions $FV^i=F(x^i)$
Initialize the normalization value $z=(z_1,\ldots,z_n)^T$ with a problem-specific procedure.
Calculate Tchebychev distances between every possible pair of weight vectors, and then select the T closest weight vectors to each weight vector. $\forall\ i=1,\ldots,N$, set $B(i)=\{i_1,\ldots,i_T\}$, where $w^{i1} \ldots w^{iT}$ are the T closest weight vectors to w^i.
Step 2 – Solution Update:
For *i* = *1,...,N*
Genetic operators: randomly select two solution k,l from $B(i)$m and then generate a new solution y from x^k and x^l using crossover and mutation operators.
Update z, $\forall\ j=1,\ldots,n$, if $z_j < f_j(y)$, then set $z_j = f_j(y)$.
Update Neighboring solutions: for each index $j \in B(i)$, if $g^{te}(y|w^j,z) <= g^{te}(x^j|w^j,z)$, then set $x^j=y$ and $FV^j=F(y^j)$.
Update NS: delete from NS all the solutions dominated by $F(y)$.
if no vector in NS dominates $F(y)$, then Add $F(y)$ to NS.
Step 3 - Stopping criteria
If $gen=gen_{max}$, then stop and output NS, otherwise $gen=gen+1$, go to Step 2.

Neighborhood size. Three neighborhood sizes T and, thus, three MOEA/D are considered. The value of this parameter is set as 1%, 1.5%, and 3% of the population size for MOEA/D T = 1%, MOEA/D T = 1.5%, and MOEA/D T = 3% respectively. These values for the neighborhood size are in line with similar works in flow shop problems of the literature (Alhindi and Zhang, 2014). The parameters of the three MOEA/Ds are tuned independently.

Representation of the solution. The solutions are encoded as a permutation of integers of length equal to number of jobs n in which each index in the vector represents the processing order in the (first) machine and the corresponding integer value represents each one of the jobs to schedule.

Initialization. The population -which is a set of size $\#P$- is initialized by applying a random procedure to generate permutations in which no integer value is repeated. Using a uniform probability distribution, each value in a solution representation is selected within the range $[1,n]$.

Crossing and mutation operators. The operator used for recombination is the well-known Partially Mapped Crossover (PMX). This crossing operator matches two selected individuals with probability p_c and has been applied in several works addressing permutation-encoded scheduling problems. Then, the mutation operator is based on Swap Mutation and it swaps two elements of the permutation. The mutation operator is applied to an individual with probability p_m. It is important to highlight that the proposed operators guarantee the feasibility of the generated solutions.

Fitness assignment and solution selection and replacement. A Mating Selection procedure to randomly select two solutions is applied. These two individuals are randomly selected from the same neighborhood (with probability 0.9) or from the whole population (with probability 0.1). Fitness is assigned considering the weights assigned to the neighborhood of the solution. And a new solution replaces an older one if it has better fitness.

4. Computational Experimentation

This section presents the results of the computational experiments performed by the proposed MOEA/Ds in a set of test instances. In particular, this section describes the test cases used in the experimentation, the methodology used for the experimental evaluation, and the main results of the computational tests.

4.1 Description of Instances used in the Experimentation

To assess the competitiveness of the MOEA/D, a set of problem instances was devised similarly to what was performed by other authors of the missing operation flow shop literature, in general (Henneberg and Neufeld, 2016), and authors that considered due-date related objective functions, in particular (Toncovich et al., 2019). Then, for getting the rest of the parameters to define each flow shop problem different statistical distributions were used. For processing times $p_{i,j}$, (i stands for machines and j for jobs), the integer values are generated following a pseudo-uniform distribution in the interval [0;100]. Given that the instances should include missing operations, the probability of missing an operation -the zero value, i.e., $p_{i,j} = 0$- has a relatively larger value than the rest of the possible processing times -integer values from the interval [1;100]- which have relatively lower values. Then, three different sets of instances are created considering a probability of skipping an operation of 5%, 10% and 20% in line with realistic values in industry. Finally, the due dates of the jobs are calculated using Equation 6.

$$d_j = round(\sum_{i \in I} p_{i,j}(1 + 3\, random)) \tag{6}$$

Equation 6 considers all the operations that have to be performed to job j plus an extra time which is randomly determined by a uniform probability distribution in the interval [0;1]. Then, this sum is rounded to the nearest integer.

Additionally, to the variation of the probability of skipping operations, different numbers of jobs and machines are used for creating the instances. Regarding the number of jobs (n), the values that were used are: 80, 120 and 150. In terms of the number of machines (m) the values that were used are 20 and 30. Finally, the names of the problem instances follows the convention $n \times m - p\% - i$, in which n is the number of jobs, m is the number of machines, $p\%$ is the probability of skipping operations, and i is an ordinal to identify problem instances with the same values of n, m, and $p\%$. For example, $20 \times 15 - 10\% - 1$ and $20 \times 15 - 10\% - 2$ represent two different problem instances of 20 jobs, 15 machines, and 10% of missing operations.

4.2 Methodology for the Computational Experimentation

This subsection presents the description of how the computational experimentation of the proposed MOEA/Ds is performed.

Implementation details. The implementation of the proposed MOEA/Ds was performed in Java, using the framework JMetal version 4.5.2 (publicly available at http://jmetal.sourceforge.net/). Adjustments were made to the original framework in two aspects. Firstly, a normalization of the objectives was introduced in the internal handling of MOEA/D since the objectives that are addressed in this article have different magnitudes and ranges. Thus, the lack of normalization can lead to a deterioration in the MOEA/D performance (Ishibuchi and Nojima, 2017). For achieving this a correction factor was used to multiply the weights. This correction factor is the relation between the best value of both objectives and is updated in every iteration. Secondly, the reference point that was used to calculate the Relative Hypervolume (RHV) was modified to correctly get the nadir point -the point conformed by the worst value of each objective within the solution of the Pareto front (Figure 1(a))- to calculate the hypervolume. In the original version, the reference point was taken from the true Pareto front or approximated Pareto front, i.e., the front that is built considering every run of each instance. As it is shown in Figure 1, this can lead to a sub representation of the solution space and, thus, affect the RHV. In the modified version, the reference point is selected considering all the Pareto fronts obtained for a certain instance.

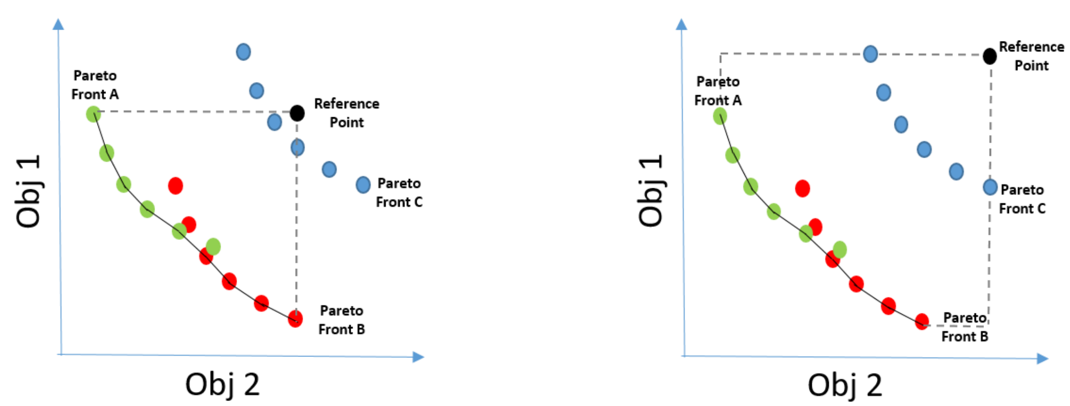

(a) Reference point used by JMetal (b) Reference point used in the modified version

Figure 1. Reference points used for computing the RHV metric.

The experimental evaluation was performed in an HP ProLiant DL380 G9 high end server with two Intel Xeon Gold 6138 processors (20 cores each) and 128 GB RAM, from the high performance computing infrastructure of National Supercomputing Center, Uruguay (Cluster-UY) (Nesmachnow and Iturriaga, 2019).

Metrics. The results of the proposed MOEA/Ds are evaluated with two standard metrics for multiobjective optimization: spread and Relative Hypervolume (RHV). Spread is a metric of diversity that evaluates the distribution of the non-dominated solutions. Thus, it assesses the capacity of correctly sampling the Pareto front. Differently to other typical metrics for distribution, such as spacing, the spread -which its formula is defined in Equation (7) (Deb, 2001)- takes into account the information about the extreme points of the true Pareto front to calculate a more accurate value of the distribution. In Equation (7), d_h^e is the distance between the extreme point of the Pareto front regarding objective *h* and the closest non-dominated solution in the computed Pareto front; d_i is the distance between the i-th non-dominated solution in the computed Pareto front and the closest neighbor non-dominated solution; and $\bar{d}$ is the average value of all d_i. *ND* and *k* are the number of non-dominated solutions and objectives respectively.

$$Spread = \frac{\sum_{h=1}^{k} d_h^e + \sum_{i=1}^{ND} |\bar{d} - d_i|}{\sum_{h=1}^{k} d_h^e + ND\,\bar{d}}. \tag{7}$$

The smaller the value of the spread, the better is the distribution of the non-dominated solutions in the calculated Pareto front. Thus, in an ideal equally spaced distribution the spread is equal to zero.

In turn, the relative hypervolume is the ratio between the volumes (in the search space of the objective functions) covered by the computed Pareto front and the true Pareto front of the problem. Thus, in an ideal situation the value of the RHV is equal to one. Therefore, RHV is a good summary metric that evaluates both the numerical accuracy, i.e., proximity of the computed Pareto front to the real Pareto front, and also the distribution of the non-dominated solutions. When the true Pareto front for a problem instance is unknown, it is estimated with all the non-dominated solutions found in all the resolutions performed for that instance.

Statistical analysis for comparison. Since the procedure of the MOEA/Ds have aleatory decisions in its functioning, the comparison is performed using adequate statistical methods after performing 30 independent executions of each version of MOEA/D for each problem instance. Then, a two-step statistical analysis is applied (Toutouh et al., 2020). These steps depend on whether the metric to study follows a normal distribution or not. On the one hand if the results of the analyzed metric of all the MOEAs follow a normal distribution, the first step is to calculate the mean value and the standard deviation (std) to typify the sample, and then use the ANOVA procedure to analyze whether there are statistically significant differences among the means. On the other hand of the metric of any of the compared MOEAs does not have a normal distribution, the first step is to calculate the median and interquartile range (IQR) to typify the sample, and then the non-parametric Kruskal-Wallis procedure is used to analyze the differences among the medians of the different algorithms.

Parameters setting. The selection of the best parametric configuration was also performed by the application of statistical analysis. This was used to set the values of the three main parameters of the studied MOEA/Ds: the population size *#P*, the crossover probability p_c and the mutation probability p_m. For the population size the tested values were 100 and 200 individuals. For the crossover probability the tested values were 0.5, 0.7 and 0.9. Finally, for the mutation probability the tested values were 0.01, 0.05 and 0.1. Thus, a total of fifteen parametric configurations were analyzed. The analysis was based on the RHV since, as aforementioned, it is a good summary metric. As a stopping condition, the maximum number of evaluations of the objective function for the executions for the parameters setting was set to 100,000. Three instances of size $n = 15$, m $m = 20$ and $\%p = 15$ were used for this analysis. These instances are different from the ones used for the normal computational experimentation of Section 4.3 to avoid bias. For each combination of instance and parametric configuration -(p_c, p_m, P)-, 50 independent executions were performed with each MOEA/D. To test the goodness of fit of the RHV results to the standard normal distribution, the Shapiro-Wilk test was used. This test determined that RHV values did not adjust to a normal distribution. Thus, the values were analyzed with the Friedman rank test, which is non-parametric, in order to determine the configuration that allowed computing the best results (Table 1). Since 15 parametric configurations were tested, this rank orders the configurations from the worst -expressed with number 1- to the best configuration -expressed with number 15-. For the MOEA/D T = 1% and MOEA/D T = 1.5%, the parametric configuration that allowed computing the best results is $p_c = 0.9$, $p_m = 0.05$, and $\#P = 200$. In the case of the MOEA/D T = 3% the used configuration is $p_c = 0.9$, $p_m = 0.1$, and $\#P = 200$. Thus, these parametric configurations are used to compute the results of Section 4.3.

Table 1. Parametric setting of the MOEA/Ds using the Friedman rank test.

Parametric configuration (p_c, p_m,#P)	**Instances**								
	Instance 1			***Instance 2***			***Instance 3***		
	T = 1%	**T = 1.5%**	**T = 3%**	**T = 1%**	**T = 1.5%**	**T = 3%**	**T = 1%**	**T = 1.5%**	**T = 3%**
(0.5,0.01,100)	1	3	1	1	1	1	1	1	1
(0.7,0.01,100)	4	4	3	2	3	3	2	3	4
(0.9,0.01,100)	3	1	4	4	2	5	3	2	5
(0.5,0.05,100)	8	7	6	8	7	12	7	8	8
(0.7,0.05,100)	9	8	8	9	9	9	9	9	9
(0.9,0.05,100)	11	6	10	10	12	11	11	10	11
(0.5,0.1,100)	10	14	13	13	16	13	15	13	14
(0.7,0.1,100)	14	11	16	18	15	17	16	14	17
(0.9,0.1,100)	12	13	12	16	11	18	17	15	16
(0.5,0.01,200)	2	2	2	3	4	2	4	5	2
(0.7,0.01,200)	5	5	5	5	5	4	5	4	3
(0.9,0.01,200)	6	10	9	6	6	6	6	6	6
(0.5,0.05,200)	7	9	7	7	8	7	8	7	7
(0.7,0.05,200)	13	16	11	11	13	10	10	12	10
(0.9,0.05,200)	18	18	17	17	18	8	18	18	13
(0.5,0.1,200)	17	12	15	14	17	16	13	17	12
(0.7,0.1,200)	16	17	14	15	14	15	12	16	15
(0.9,0.1,200)	15	15	18	12	10	14	14	11	18

4.3 Results of Test Instances

This subsection describes the result of the computational experimentation.

Metrics for multi objective optimization. Tables 2 and 3 show the results obtained by the MOEA(Ds of the RHV and spread respectively. The Tables show from left to right and each table reports for each instance and for the corresponding metric computed for each MOEA: the test used to study if the differences among the medians or averages are statistically significant (i.e., Kruskal-Wallis for analyzing medians and ANOVA for analyzing maverages); and the smallest or minimal value, the median or average value, the largest or maximal value, and the measure used for representing dispersion of the results (standard deviation for normal distributions or the interquartile range for non-parametric distributions).

In the aforementioned Tables 2 and 3, data of special interest for this study was highlighted. The best results for each metric are shown in bold. Some results were marked with an asterisk to indicate the cases in which the statistical test verified a significant statistical difference with respect to the rest of the MOEA/Ds, considering a confidence level of 95% (p-value of this statistical test is less than 0.05).

According to Table 2, MOEA/D with T = 3% outperformed the other two MOEA/D in all the instances in terms of mean/median RHV. In terms of maximum RHV MOEA/D T = 3% present better results for all the instances except for instance 80×20-20-2. The best global RHV result was obtained for instance 150×30-5-2 by MOEA/D T = 3% (0.9965). Additionally, MOEA/D with T = 3% obtained RHV values larger than 0.9 for eight instances.

Table 2. Results of the RHV metric of each MOEA/D.

Instance	Test	T = 1%				T = 1.5%				T = 3%			
		min	*mean/ median*	*max*	*σ/IQR*	*min*	*mean/ median*	*max*	*σ/IQR*	*min*	*mean/ median*	*max*	*σ/IQR*
120×20-10-1	ANOVA	0.2137	0.3943	0.6320	0.1072	0.1683	0.4209	0.6535	0.1081	0.3536	***0.5694**	**0.8340**	0.1370
120×20-10-2	ANOVA	0.1721	0.4137	0.6037	0.1065	0.1217	0.4505	0.7698	0.1505	0.3679	***0.5834**	**0.9420**	0.1489
120×30-10-1	ANOVA	0.1948	0.5051	0.8117	0.1236	0.1226	0.5555	0.8100	0.1507	0.3930	***0.6973**	**0.9541**	0.1306
120×30-10-2	ANOVA	0.2497	0.3982	0.5823	0.0880	0.1686	0.3694	0.6985	0.0999	0.3166	***0.5609**	**0.8356**	0.1163
150×30-10-1	ANOVA	0.1762	0.3616	0.6495	0.1114	0.1301	0.3581	0.5693	0.1243	0.3479	***0.6035**	**0.9435**	0.1336
150×30-10-2	ANOVA	0.0974	0.4160	0.5882	0.1165	0.1914	0.4380	0.7384	0.1263	0.3802	***0.6213**	**0.8579**	0.1218
40×20-10-1	Kruskal-Wallis	0.4028	0.6087	0.7489	0.0826	0.4133	0.6232	0.7142	0.0686	0.4904	**0.6910**	**0.7996**	0.1036
40×20-10-2	Kruskal-Wallis	0.5721	0.7348	0.8232	0.0751	0.6413	0.7384	0.8001	0.0716	0.6816	**0.7732**	**0.8490**	0.0756
80×20-10-1	Kruskal-Wallis	0.2605	0.4288	0.7723	0.1356	0.2261	0.4527	0.8748	0.1467	0.1761	**0.5876**	**0.8615**	0.2324
80×20-10-2	ANOVA	0.2490	0.4574	0.6212	0.0970	0.2098	0.4703	0.6727	0.1220	0.2422	***0.5752**	**0.9427**	0.1570
120×20-20-1	ANOVA	0.1165	0.4281	0.6905	0.1457	0.1547	0.3967	0.8355	0.1535	0.2971	***0.5277**	**0.7672**	0.1145
120×20-20-2	Kruskal-Wallis	0.2076	0.3596	0.8598	0.2066	0.1428	0.4591	0.6902	0.1728	0.3883	**0.6364**	**0.8755**	0.1899
120×30-20-1	ANOVA	0.2111	0.4218	0.7178	0.1150	0.2320	0.4827	0.7145	0.1210	0.2848	***0.6117**	**0.8557**	0.1336
120×30-20-2	Kruskal-Wallis	0.1981	0.4322	0.6628	0.1403	0.2722	0.4545	0.6593	0.1175	0.3602	**0.5581**	**0.8770**	0.1875
150×30-20-1	ANOVA	0.1172	0.3569	0.5950	0.1115	0.0906	0.4231	0.8552	0.1716	0.2424	***0.5447**	**0.9471**	0.1524
150×30-20-2	ANOVA	0.0745	0.3399	0.5234	0.1093	0.1874	0.4254	0.7607	0.1384	0.2210	***0.5845**	**0.8752**	0.1699
40×20-20-1	Kruskal-Wallis	0.5281	0.6686	0.7860	0.0752	0.4566	0.6765	0.8168	0.1363	0.5357	**0.7248**	**0.8488**	0.0519
40×20-20-2	ANOVA	0.5086	0.6600	0.8193	0.0717	0.5320	0.6524	0.7958	0.0668	0.5877	***0.7066**	**0.8439**	0.0695
80×20-20-1	ANOVA	0.2665	0.5352	0.7416	0.1037	0.2448	0.5182	0.8238	0.1388	0.4182	***0.6520**	**0.8961**	0.1282
80×20-20-2	ANOVA	0.1839	0.4158	0.6595	0.1240	0.1529	0.4546	**0.8177**	0.1585	0.1916	***0.5710**	0.7837	0.1235
120×20-5-1	ANOVA	0.1892	0.4091	0.5993	0.1051	0.1308	0.4192	0.7382	0.1292	0.2214	***0.5466**	**0.8522**	0.1426
120×20-5-2	ANOVA	0.1974	0.3869	0.5886	0.0921	0.2223	0.3830	0.6258	0.1044	0.3372	***0.5324**	**0.9035**	0.1280
120×30-5-1	Kruskal-Wallis	0.1714	0.3356	0.6376	0.1306	0.1899	0.3672	0.6127	0.1451	0.3692	**0.4889**	**0.9599**	0.1520
120×30-5-2	ANOVA	0.1230	0.4138	0.6594	0.1268	0.2140	0.4476	0.6640	0.1143	0.1627	***0.5529**	**0.7768**	0.1483
150×30-5-1	ANOVA	0.0686	0.3112	0.6907	0.1364	0.1380	0.3327	0.6437	0.1156	0.1686	***0.4875**	**0.8241**	0.1525
150×30-5-2	ANOVA	0.2156	0.4371	0.6505	0.1301	0.1547	0.4464	0.8364	0.1513	0.2565	***0.5991**	**0.9965**	0.1852
40×20-5-1	ANOVA	0.4058	0.5758	0.7668	0.0803	0.4795	0.6034	0.7277	0.0753	0.5251	***0.6582**	**0.8377**	0.0758
40×20-5-2	ANOVA	0.4724	0.6087	0.7334	0.0654	0.4352	0.5927	0.7446	0.0649	0.5358	**0.6309**	**0.7941**	0.0563
80×20-5-1	ANOVA	0.2048	0.3813	0.6068	0.1005	0.2889	0.4664	0.6755	0.0929	0.2200	***0.5524**	**0.7456**	0.1325
80×20-5-2	ANOVA	0.2467	0.5138	0.6971	0.1123	0.2963	0.5232	0.8022	0.1200	0.3355	***0.6248**	**0.8486**	0.1500

In terms of the spread metric for multi objective optimization, MOEA/D T = 1% obtained the best median/mean value in 14 out of 30 instances while MOEA/D T = 1.5% in the other 16 instances. Regarding the smallest spread value, MOEA/D with T = 1% computed the best results in 16 instances, MOEA/D T = 1.5% in 12 instances, and MOEA/D with T = 3% only in 3 instances. The overall smallest value is 1.0000 and is obtained for instances 120×20-10-2, 120×30-10-1, 120×20-20-1 by MOEA/D T = 1%, instance 80×20-5-1 for MOEA/D T = 1.5%, and instances 120×20-20-1 and 80×20-5-2 by MOEA/D T = 3%. The same minimal spread value of 1.0000 is obtained by MOEA/D with T = 1% and MOEA/D T = 3% for instance 120×20-20-1.

Table 3. Results of the spread metric for each MOEA/D.

Instance	Test	T = 1%				T = 1.5%				T = 3%			
		min	*mean/ median*	*max*	*σ/IQR*	*min*	*mean/ median*	*max*	*σ/IQR*	*min*	*mean/ median*	*max*	*σ/IQR*
120×20-10-1	ANOVA	**1.0812**	**1.2156**	1.4356	0.0900	1.0826	1.2530	1.4944	0.0959	1.1781	1.3386	1.4863	0.0856
120×20-10-2	Kruskal-Wallis	**1.0000**	1.2302	1.4897	0.1087	1.0673	**1.2247**	1.4879	0.0946	1.0377	1.2905	1.7373	0.1404
120×30-10-1	Kruskal-Wallis	**1.0000**	**1.1896**	1.4421	0.0472	1.0502	1.2185	1.4163	0.1361	1.0725	1.2413	1.5799	0.1174
120×30-10-2	ANOVA	**1.0562**	1.2663	1.4243	0.0802	1.0816	**1.2487**	1.4513	0.0755	1.1863	1.3248	1.4428	0.0712
150×30-10-1	ANOVA	1.0663	1.2616	1.4854	0.1191	**1.0497**	**1.2350**	1.3747	0.0889	1.1291	1.3381	1.5159	0.1025
150×30-10-2	ANOVA	1.0757	1.2113	1.3570	**0.0769**	1.0750	**1.2053**	1.3941	0.0873	**1.0624**	1.2714	1.4391	0.1117
40×20-10-1	ANOVA	**1.2695**	**1.4835**	1.7227	0.1022	1.3386	1.4852	1.6187	0.0806	1.3166	1.4983	1.7006	0.0889
40×20-10-2	Kruskal-Wallis	1.4262	1.5141	1.6249	0.0824	1.3925	**1.4891**	1.6249	0.0627	**1.2993**	1.5049	1.5510	0.0742
80×20-10-1	ANOVA	1.1081	1.2571	1.4846	0.0941	**1.0120**	**1.2324**	1.5275	0.1066	1.0371	1.3003	1.5767	0.1216
80×20-10-2	ANOVA	1.0667	1.3012	1.4274	0.0894	**1.0465**	**1.2805**	1.4325	0.1077	1.1096	1.3633	1.5115	0.0984
120×20-20-1	ANOVA	**1.0000**	1.2498	1.5529	0.1156	1.0376	**1.2244**	1.5637	0.1198	1.0000	1.2663	1.4500	0.1114
120×20-20-2	ANOVA	1.0759	1.2288	1.3752	0.0808	**1.0227**	**1.2282**	1.4383	0.0939	1.1336	1.3161	1.5896	0.1076
120×30-20-1	Kruskal-Wallis	**1.0863**	1.2589	1.4157	0.1172	1.0968	1.3133	1.5632	0.1415	1.2254	**1.3119**	1.5457	0.1806
120×30-20-2	ANOVA	1.1507	**1.2566**	1.4481	0.0658	1.1336	1.2650	1.4352	0.0695	**1.1189**	1.3233	1.5786	0.1156
150×30-20-1	ANOVA	**1.0309**	**1.1867**	1.3424	0.0797	1.0784	1.2180	1.4777	0.0995	1.0837	1.2689	1.5638	0.0973
150×30-20-2	ANOVA	**1.0540**	**1.1835**	1.3395	0.0661	1.0697	1.1892	1.3996	0.0821	1.1408	1.2734	1.5401	0.1045
40×20-20-1	ANOVA	1.2600	**1.3865**	1.5643	0.0788	**1.1899**	1.4007	1.6305	0.1086	1.1997	1.4142	1.5797	0.0882
40×20-20-2	ANOVA	**1.3498**	**1.4821**	1.6159	0.0646	1.3842	1.4840	1.5969	0.0614	1.3729	1.5035	1.6275	0.0685
80×20-20-1	ANOVA	**1.1570**	1.3676	1.5432	0.1068	1.1742	**1.3499**	1.5492	0.0932	1.1667	1.3985	1.6187	0.1168
80×20-20-2	ANOVA	1.1080	1.2785	1.4348	0.0835	**1.0415**	***1.2322**	1.4446	0.0859	1.1090	1.3186	1.5793	0.1145
120×20-5-1	Kruskal-Wallis	1.0718	**1.2513**	1.4447	0.1058	**1.0383**	1.2747	1.3984	0.0890	1.1308	1.3462	1.4278	0.0852
120×20-5-2	ANOVA	**1.0567**	**1.2167**	1.3956	0.0879	1.0934	1.2190	1.4096	0.0748	1.1369	1.2787	1.5498	0.0968
120×30-5-1	ANOVA	**1.0309**	**1.2156**	1.4131	0.0759	1.0919	1.2408	1.4106	0.0805	1.1292	1.2952	1.5305	0.1114
120×30-5-2	ANOVA	**1.0491**	1.2577	1.4182	0.1035	1.1144	**1.2476**	1.4068	0.0702	1.1658	1.3168	1.4915	0.0809
150×30-5-1	Kruskal-Wallis	1.0873	**1.1717**	1.3206	0.0724	**1.0814**	1.1867	1.4270	0.1168	1.1428	1.2542	1.5921	0.1872
150×30-5-2	Kruskal-Wallis	**1.0481**	1.1632	1.2679	0.0658	1.0672	**1.1574**	1.3361	0.0627	1.0930	1.2261	1.9196	0.1037
40×20-5-1	Kruskal-Wallis	1.2974	1.4694	1.6993	0.1144	**1.1350**	**1.4585**	1.6101	0.0957	1.1722	1.4652	1.6951	0.1432
40×20-5-2	ANOVA	**1.2594**	1.4698	1.6643	0.0905	1.2822	**1.4371**	1.5852	0.0945	1.2825	1.4637	1.6407	0.0883
80×20-5-1	ANOVA	1.0297	**1.2645**	1.4945	0.0969	**1.0000**	1.3031	1.5836	0.1117	1.1179	1.3459	1.6324	0.1350
80×20-5-2	ANOVA	1.1654	1.3511	1.5715	0.1036	1.1228	**1.3299**	1.5385	0.1125	**1.0000**	1.3493	1.5745	0.1299

Distance between the ideal vector and the best trade-off or compromising solution. To explain the calculation of this metric, Figure 2 is introduced. This Figure shows a generic minimization problem with 2 objective functions $f_1(x)$and $f_2(x)$, and the ideal vector or solution which is represented with a yellow point. That point is obtained by combining the best values achieved in any execution for each objective function and, thus, it is an unattainable point. Then, within the calculated Pareto front, the best compromising or trade-off solution is marked with a red point. This solution is obtained by selecting the solution of the Pareto front that minimizes the distance to the ideal solution (yellow point), using in this case the Euclidean distance. Then, Table 4 shows the Euclidean distances between the best compromising solution obtained by each MOEA and the ideal solution in each instance. These distances are expressed in terms of percentage difference with respect to the ideal vector considering each of the objective functions, i.e., Total Tardiness (δ_T) and Makespan (δ_C) respectively, and finally a global deviation Δ, which is obtained through Equation (8).

$$\Delta = \sqrt{\sum_{o \in O} \left(\frac{value - ideal_o}{ideal_o}\right)^2} \quad (8)$$

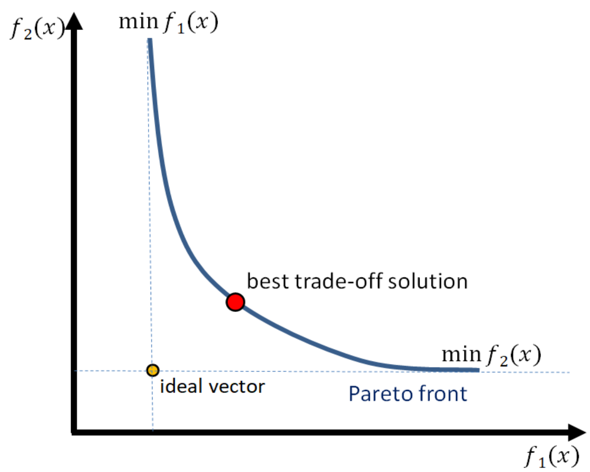

Figure 2. Representation of the ideal solution or vector of the instance and the best compromising solution achieved by each algorithm.

Analyzing the results of the distance between the ideal solution and the solution with the best-trade-off shown in Table 4, it can be concluded that the three MOEAs obtain, in general, accurate solutions for most of the instances. The exceptions are compromising solutions obtained in the instances with the smallest number of jobs (type 40x20). In those instances the distance to the value of the objective total tardiness is much larger, contributing with a larger overall deviation Δ. Conversely, for this subset of instances the distance to the makespan is much smaller and in line with the values obtained for the rest of the instances.

Regarding the comparison among the MOEA/Ds, similar to the results of the RHV metric, the situation is more favorable to the MOEA/D T = 3%. Indeed, MOEA/D T = 3% outperforms the other two algorithms in 22 out of 30 instances in terms of difference from the ideal solution for total tardiness, 23 out of 30 instances in terms of difference from the ideal solution for makespan, and 22 out of 30 instances in the overall deviation. MOEA/D T = 1% outperforms the other two algorithms in 8 out of 30 instances in terms of difference from the ideal solution for total tardiness, and 8 out of 30 instances in the overall deviation while MOEA/D T = 1% obtains the compromising solution with the smallest distance to the ideal vector in terms of makespan in 8 out of 30 instances.

The solution with the smallest distances were all obtained by MOEA/D T = 3%: in terms of total tardiness is 0.13% for instance 120×20-10-1, in terms of makespan is 0.01% for instance 120×30-10-1, and 0.39% in terms of overall distance for instance 150×30-5-2. MOEA/D T = 3% also outperformed the other two when considering the average values.

Table 4. Distance of the best trade-off solution obtained with MOEA/D to the ideal vector.

Instance	T = 1%			T = 1.5%			T = 3%		
	δ_T	$\delta_{C_{max}}$	Δ	δ_T	$\delta_{C_{max}}$	Δ	δ_T	$\delta_{C_{max}}$	Δ
120×20-10-1	2.86%	1.51%	3.23%	4.08%	1.07%	4.22%	**0.13%**	**1.06%**	**1.07%**
120×20-10-2	3.45%	1.46%	3.74%	1.60%	1.33%	2.08%	**1.07%**	**0.77%**	**1.31%**
120×30-10-1	1.26%	1.02%	1.62%	1.58%	0.87%	1.80%	**0.99%**	**0.01%**	**0.99%**
120×30-10-2	6.26%	1.84%	6.52%	3.13%	1.45%	3.46%	**1.25%**	**1.25%**	**1.77%**
150×30-10-1	1.36%	1.85%	2.30%	3.84%	1.07%	3.99%	**0.85%**	**0.38%**	**0.93%**
150×30-10-2	3.83%	1.54%	4.13%	3.55%	0.51%	3.59%	**1.87%**	**0.46%**	**1.93%**
40×20-10-1	36.91%	2.35%	36.98%	30.98%	2.42%	31.08%	**27.57%**	**2.26%**	**27.67%**
40×20-10-2	**88.02%**	2.31%	**88.05%**	92.77%	2.94%	92.82%	101.70%	**2.01%**	101.72%
80×20-10-1	3.36%	1.30%	3.60%	3.09%	0.24%	3.10%	**2.25%**	**0.72%**	**2.37%**
80×20-10-2	5.52%	1.94%	5.85%	5.24%	1.74%	5.53%	**0.82%**	**0.49%**	**0.96%**
120×20-20-1	**2.22%**	1.82%	**2.87%**	3.51%	**0.05%**	3.51%	3.83%	0.54%	3.87%
120×20-20-2	**0.53%**	0.72%	**0.90%**	1.32%	1.93%	2.34%	1.31%	**0.45%**	1.38%
120×30-20-1	1.16%	1.46%	1.87%	1.23%	1.41%	1.87%	**0.36%**	**0.82%**	**0.90%**
120×30-20-2	3.60%	1.58%	3.93%	5.05%	1.08%	5.16%	**2.22%**	**0.62%**	**2.31%**
150×30-20-1	1.98%	1.75%	2.65%	1.65%	0.53%	1.73%	**0.15%**	**0.38%**	**0.41%**
150×30-20-2	4.01%	1.58%	4.31%	2.71%	0.82%	2.83%	**0.45%**	**0.62%**	**0.77%**
40×20-20-1	**79.92%**	2.27%	**79.95%**	89.00%	**1.43%**	89.01%	86.28%	1.81%	86.30%
40×20-20-2	**52.10%**	4.23%	**52.28%**	70.18%	3.25%	70.25%	60.59%	**3.15%**	60.67%
80×20-20-1	3.15%	2.54%	4.05%	3.97%	1.89%	4.40%	**2.27%**	**1.28%**	**2.61%**
80×20-20-2	4.41%	2.46%	5.05%	3.18%	**1.51%**	3.52%	**1.43%**	2.08%	**2.52%**
120×20-5-1	2.37%	1.69%	2.91%	1.78%	1.05%	2.07%	**1.46%**	**0.84%**	**1.68%**
120×20-5-2	3.36%	1.41%	3.64%	1.58%	1.99%	2.54%	**0.18%**	**0.61%**	**0.63%**
120×30-5-1	5.22%	1.06%	5.33%	3.98%	1.51%	4.26%	**1.21%**	**0.51%**	**1.31%**
120×30-5-2	4.35%	1.22%	4.52%	3.71%	**1.06%**	3.86%	**2.07%**	1.15%	**2.37%**
150×30-5-1	**1.86%**	1.23%	**2.23%**	2.49%	0.91%	2.65%	2.34%	**0.45%**	2.38%
150×30-5-2	3.12%	0.94%	3.26%	1.26%	0.78%	1.48%	**0.37%**	**0.13%**	**0.39%**
40×20-5-1	**24.83%**	2.56%	**24.97%**	25.31%	2.59%	25.45%	36.04%	**1.30%**	36.07%
40×20-5-2	**42.50%**	2.43%	**42.57%**	60.00%	**2.08%**	60.04%	54.82%	2.28%	54.87%
80×20-5-1	4.18%	1.90%	4.59%	3.37%	**1.43%**	3.66%	**1.98%**	1.60%	**2.55%**
80×20-5-2	4.31%	1.39%	4.52%	3.00%	**0.85%**	3.12%	**2.38%**	0.94%	**2.56%**
Average	13.40%	1.78%	13.75%	14.60%	1.39%	14.85%	13.34%	1.03%	13.57%

Results for the consolidated Pareto fronts. The consolidated Pareto fronts are obtained from all the non-dominated solutions obtained by each MOEA for each instance of the problem considering the 30 independent executions. Table 5 presents the results of this metric**.**

Considering RHV, MOEA/D T = 3% obtained a better consolidated Pareto front in 24 out of 30 instances, MOEA/D T = 1.5% in 4 out of 30 instances and MOEA/D T = 1% in the other two instances. The highest value of RHV for the consolidated Pareto front is 0.8767 and is achieved by MOEA/D T = 3% for instance 150×30-10-1.

Once again, the performance of the MOEA/D T = 3% to achieve proper distribution and spacing of non-dominated solutions in the computed Pareto fronts is less effective in comparison to the other algorithms. Considering spread, MOEA/D T = 1% obtained a better consolidated Pareto front in 14 out of 30 instances, MOEA/D T = 1.5% in 11 out of 30 instances and MOEA/D T = 3% in the other five instances. The minimal value of spread for the consolidated Pareto front is 1.0830 and is achieved by MOEA/D T = 1% for instance 120×20-10-1.

Table 5. Results of the consolidated Pareto fronts metric for each MOEA/D.

Instance	T = 1%		T = 1.5%		T = 3%	
	RHV	spread	RHV	spread	RHV	spread
120×20-10-1	0.433	**1.083**	0.352	1.2636	**0.6468**	1.4582
120×20-10-2	0.4344	**1.1771**	0.3733	1.2118	**0.5984**	1.3648
120×30-10-1	0.5633	**1.1601**	0.5799	1.3244	**0.627**	1.2859
120×30-10-2	0.3606	1.2356	0.2584	**1.1354**	**0.7418**	1.3055
150×30-10-1	0.3218	1.2532	0.4565	**1.2479**	**0.8767**	1.4589
150×30-10-2	0.4908	1.3435	0.4216	1.1748	**0.6175**	**1.1188**
40×20-10-1	0.5652	**1.4595**	0.6511	1.5043	**0.6965**	1.4807
40×20-10-2	0.6184	**1.4375**	**0.7398**	1.4439	0.6816	1.5104
80×20-10-1	**0.4894**	1.2413	0.4468	1.2335	0.3533	**1.1423**
80×20-10-2	0.272	1.3467	0.527	**1.2535**	**0.5982**	1.3165
120×20-20-1	**0.4819**	1.2753	0.4205	1.2628	0.4356	**1.2619**
120×20-20-2	0.2076	1.2062	0.1428	**1.1225**	**0.8527**	1.5896
120×30-20-1	0.3034	1.3634	0.4445	**1.2287**	**0.7096**	1.2543
120×30-20-2	0.4407	**1.2099**	0.4765	1.2711	**0.5971**	1.324
150×30-20-1	0.353	**1.1309**	0.4353	1.2217	0.4561	1.3687
150×30-20-2	0.3582	**1.1903**	0.4216	1.1979	**0.6615**	1.2338
40×20-20-1	0.7342	**1.304**	0.6879	1.4372	**0.7628**	1.4314
40×20-20-2	0.7119	1.6029	**0.7434**	**1.4219**	0.7047	1.5426
80×20-20-1	0.5304	1.3902	0.3832	**1.1742**	**0.8207**	1.5011
80×20-20-2	0.2724	**1.2008**	0.4807	1.2072	**0.6059**	1.2043
120×20-5-1	0.3741	**1.3091**	0.4944	1.3984	**0.7146**	1.3167
120×20-5-2	0.3437	1.3075	0.2223	**1.0934**	**0.4981**	1.3279
120×30-5-1	0.4035	1.2746	0.4578	1.3507	**0.5665**	**1.2059**
120×30-5-2	0.4213	1.2981	0.2828	**1.1935**	**0.5576**	1.2516
150×30-5-1	0.2083	**1.1264**	0.2824	1.1403	**0.7424**	1.4164
150×30-5-2	0.5407	**1.1052**	0.3578	1.1582	**0.6204**	1.2391
40×20-5-1	0.4964	1.4105	0.4795	**1.2952**	**0.7376**	1.6269
40×20-5-2	0.4947	1.527	**0.6735**	1.5401	0.5358	**1.4688**
80×20-5-1	0.4412	1.3179	0.2889	**1.2956**	**0.6115**	1.4614
80×20-5-2	0.6879	**1.2242**	**0.8022**	1.5385	0.4868	1.4336

As a graphic presentation of the general results, Figure 3 is introduced. In this Figure, the consolidated Pareto fronts are presented for three representative cases. In the case of the instance 80x20-20-1, the Pareto front computed by MOEA/D T = 3% dominates the results of the other two MOEAs. MOEA/D T = 1% presents a good distribution of solutions. In Figure 4 this is even more evident, having a larger distance between some of the solutions of the Pareto front of MOEA/D T = 3% and the solutions of the other two MOEAs, especially MOEA/D T = 1%. but SPEA2 was able to better sample solutions with the lowest values of the makespan objective. In 40x20-10-1, the performance among the MOEAs is more similar. This type of instance, i.e., 40x20, is the type in which the worst distances to the ideal vector are achieved (Table 4).

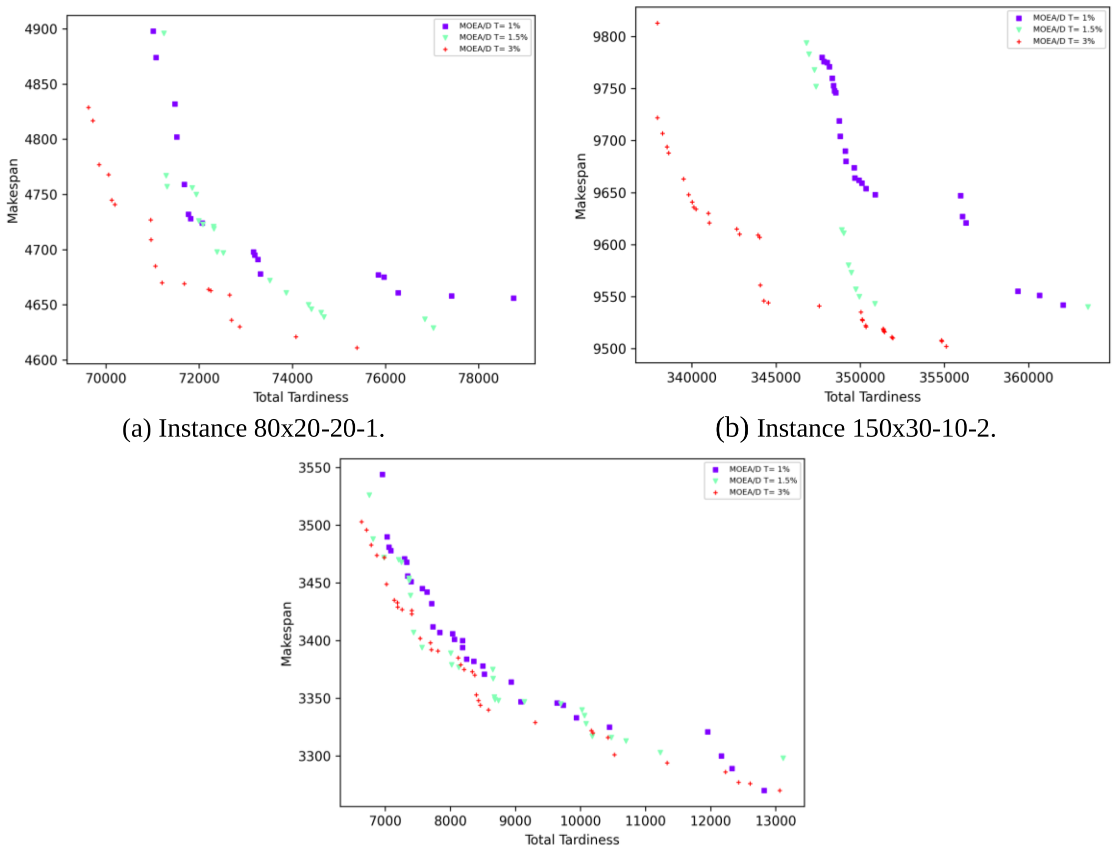

(a) Instance 80x20-20-1.

(b) Instance 150x30-10-2.

(c) Instance 40x20-10-1.

Figure 3. Pareto fronts of MOEA/Ds for representative problem instances.

Comparison to baseline NSGAII and SPEA2 results. Tables 6-8 present the comparison with two state-of-art metaheuristic NSGAII and SPEA2 on a subset of instances. The NSGAII and SPEA2 were developed in Rossit et al. (2021c) and are used as baseline for comparison, since they applied the same evolutionary operators as the proposed MOEA/Ds. Using the values in Rossit et al. (2021c) as a baseline, Table 6 and 7 compare the RHV and spread respectively. Regarding RHV values of Table 6, no highest value was found to be significantly different to the rest of the values of RHV, applying the statistical tests. MOEA/D using T = 3% outperformed the rest of the algorithms in 12 out of 24 instances, whereas NSGAII outperforms the other four algorithms in 8 out of 24 instances. Finally, SPEA2 achieves the highest RHV in 4 out of 24 instances. MOEA/D T = 1%, MOEA/D T = 1.5% seem not to be competitive in terms of RHV. The best RHV is 0.6968 and is obtained for instance 80×20-5-2 by NSGAII.

Table 6. RHV comparison with baseline NSGAII and SPEA2.

Instance	Test	MOEA/D T = 1%		MOEA/D T = 1.5%		MOEA/D T = 3%		NSGAII		SPEA2	
		Mean /median	***σ/IQR***	***mean/ median***	***σ/IQR***	***mean/ median***	***σ/IQR***	***Mean /median***	***σ/IQR***	***mean/ median***	***σ/IQR***
120×20-10-1	Kruskal-Wallis	0.3764	0.1510	0.4024	0.1169	0.4962	0.1802	**0.5781**	0.1315	0.4747	0.1831
120×20-10-2	ANOVA	0.3726	0.0929	0.4049	0.1308	0.5204	0.1297	**0.5727**	0.1336	0.5109	0.1348
120×30-10-1	ANOVA	0.4115	0.1007	0.4526	0.1228	0.568	0.1064	0.5688	0.1071	**0.5814**	0.1612
120×30-10-2	ANOVA	0.4189	0.0863	0.3918	0.098	**0.5749**	0.1137	0.5214	0.1158	0.4988	0.1181
150×30-10-1	ANOVA	0.3372	0.1013	0.3331	0.112	**0.5537**	0.1197	0.5118	0.1222	0.4879	0.1525
150×30-10-2	ANOVA	0.3932	0.1102	0.414	0.1194	**0.5872**	0.1151	0.5838	0.1324	0.5812	0.1264
80×20-10-1	Kruskal-Wallis	0.4803	0.1377	0.5012	0.1445	0.6244	0.2111	**0.6540**	0.1518	0.6042	0.1946
80×20-10-2	ANOVA	0.4646	0.0865	0.475	0.1097	**0.5694**	0.1394	0.5612	0.0938	0.5246	0.1322
120×20-20-1	ANOVA	0.4392	0.1409	0.4082	0.1427	0.5251	0.1036	0.5440	0.129	**0.5517**	0.0958
120×20-20-2	Kruskal-Wallis	0.4329	0.1961	0.5133	0.1373	**0.6717**	0.1675	0.6281	0.1697	0.6138	0.1828
120×30-20-1	ANOVA	0.3603	0.0903	0.408	0.0947	**0.5108**	0.1044	0.4516	0.117	0.4707	0.1515
120×30-20-2	Kruskal-Wallis	0.417	0.1195	0.4343	0.0826	0.5193	0.1488	**0.5691**	0.165	0.5427	0.1384
150×30-20-1	ANOVA	0.413	0.1061	0.4752	0.1591	**0.5884**	0.1386	0.5728	0.1181	0.5495	0.1027
150×30-20-2	ANOVA	0.3521	0.0927	0.4223	0.1145	**0.5525**	0.1382	0.5129	0.1167	0.512	0.1281
80×20-20-1	ANOVA	0.482	0.0713	0.4711	0.0972	0.568	0.0904	0.5876	0.1133	**0.6027**	0.1016
80×20-20-2	ANOVA	0.4566	0.1083	0.4958	0.1461	**0.5988**	0.1062	0.5904	0.1355	0.5767	0.1458
120×20-5-1	ANOVA	0.4426	0.0943	0.4511	0.113	0.5648	0.1269	**0.6065**	0.1441	0.5262	0.1257
120×20-5-2	ANOVA	0.4224	0.0827	0.424	0.0882	**0.5493**	0.1071	0.5467	0.1167	0.5147	0.0997
120×30-5-1	Kruskal-Wallis	0.331	0.1281	0.3618	0.1432	0.4810	0.1491	0.4855	0.2275	**0.4959**	0.2124
120×30-5-2	ANOVA	0.4221	0.115	0.4531	0.1026	**0.5485**	0.136	0.5108	0.1032	0.5241	0.1265
150×30-5-1	ANOVA	0.3116	0.1363	0.3331	0.1156	0.4878	0.1524	0.4197	0.1271	0.4332	0.119
150×30-5-2	ANOVA	0.4518	0.1127	0.4592	0.1307	0.5908	0.1578	**0.6006**	0.1329	0.5285	0.1048
80×20-5-1	ANOVA	0.4223	0.0892	0.4984	0.0813	0.5718	0.1163	**0.607**	0.1318	0.5821	0.1369
80×20-5-2	ANOVA	0.5547	0.0801	0.5622	0.097	0.6386	0.1101	**0.6968**	0.0914	0.6745	0.1122

Concerning spread values, results in Table 7 indicate that the best algorithms are MOEA/D using T=1% and T=1.5%. Using T=1% outperformed the other four MOEAs in 12 out of 24 instances and using T=1.5% in 10 out of 24 instances. Finally, SPEA2 achieves the best value in 2 instances. The overall smallest value is 1.1717 and is obtained by MOEA/D T=1% in instance 150×30-5-1. Only the value of MOEA/D T=1.5% in instance 80×20-20-2 was found to be statistically different.

Table 8 presents the distance to the ideal vector similarly to Table 4. In terms of total tardiness, MOEA/D T=1% is able to compute the solution with the smallest difference in 2 out of 24 instances, MOEA/D T=3% in 12 out of 24 instances, NSGAII in 7 out of 24 instances and finally SPEA2 in 3 out of 24 instances. In terms of makespan the results are more balanced among MOEA/D T=3%, NSGAII and SPEA2 obtaining 6, 9 and 8 out of 24 instances respectively. The overall distance best results are also mostly concentrated between MOEA/D T=3%, NSGAII and SPEA2 achieving the best result in 12, 6 and 4 out of 24 instances respectively. The minimum distance for total tardiness is 0.15% and is achieved by MOEA/D T=3% for instance 150×30-20-1. Regarding makespan the smallest value is 0.23% and is reached by NSGAII for instance 120×20-5-2. Finally, the overall distance smallest value is 0.41% obtained by MOEA/D T=3% for instance 150×30-20-1.

Table 7. Spread comparison with baseline NSGAII and SPEA2.

Instance	Test	MOEA/D T = 1%		MOEA/D T = 1.5%		MOEA/D T = 3%		NSGAII		SPEA2	
		mean/ median	*σ/IQR*	*mean /median*	*σ/IQR*	*mean /median*	*σ/IQR*	*mean/ median*	*σ/IQR*	*mean/ median*	*σ/IQR*
120×20-10-1	ANOVA	**1.2054**	0.0871	1.2379	0.0928	1.3122	0.0824	1.3777	0.1009	1.3005	0.0742
120×20-10-2	Kruskal-Wallis	**1.2150**	0.1063	1.2195	0.0800	1.2811	0.1764	1.3434	0.1298	1.2620	0.0643
120×30-10-1	ANOVA	**1.2256**	0.0861	1.2492	0.0982	1.2637	0.1099	1.3423	0.0993	1.2745	0.0940
120×30-10-2	ANOVA	1.2663	0.0802	1.2487	0.0755	1.3248	0.0712	1.3769	0.0977	**1.2653**	0.0674
150×30-10-1	Kruskal-Wallis	1.2131	0.1495	**1.2101**	0.1086	1.3153	0.0984	1.3051	0.0683	1.2453	0.0771
150×30-10-2	ANOVA	1.1879	0.0696	**1.1817**	0.0775	1.2431	0.1065	1.2956	0.0981	1.2184	0.0800
80×20-10-1	Kruskal-Wallis	1.2775	0.1431	**1.2440**	0.1422	1.3489	0.1433	1.4500	0.1305	1.2674	0.1075
80×20-10-2	Kruskal-Wallis	1.2982	0.0919	1.2766	0.1582	1.3420	0.1011	1.3855	0.1016	**1.2725**	0.1113
120×20-20-1	ANOVA	1.2464	0.1049	**1.2268**	0.1159	1.2608	0.1122	1.3635	0.0945	1.2960	0.0959
120×20-20-2	ANOVA	1.2288	0.0808	**1.2282**	0.0939	1.3161	0.1076	1.3341	0.0929	1.2686	0.0805
120×30-20-1	Kruskal-Wallis	**1.2003**	0.1135	1.2442	0.0932	1.2897	0.1014	1.2770	0.1184	1.2347	0.0605
120×30-20-2	Kruskal-Wallis	**1.2539**	0.0853	1.2573	0.1029	1.2712	0.1451	1.3694	0.0913	1.2736	0.0944
150×30-20-1	ANOVA	**1.1867**	0.0797	1.2180	0.0995	1.2689	0.0973	1.2914	0.0641	1.2180	0.0505
150×30-20-2	ANOVA	**1.1867**	0.0797	1.2180	0.0995	1.2689	0.0973	1.2914	0.0641	1.2180	0.0505
80×20-20-1	ANOVA	1.2928	0.1072	**1.2796**	0.0869	1.3123	0.1175	1.3530	0.0983	1.3024	0.0701
80×20-20-2	ANOVA	1.2852	0.0952	***1.2328**	0.0883	1.2829	0.1027	1.3702	0.1181	1.2847	0.0835
120×20-5-1	Kruskal-Wallis	**1.2349**	0.0893	1.2438	0.1264	1.3188	0.1216	1.3367	0.1402	1.2402	0.1037
120×20-5-2	Kruskal-Wallis	1.2091	0.0719	**1.2075**	0.0805	1.2601	0.0985	1.2883	0.0872	1.2199	0.0676
120×30-5-1	ANOVA	**1.2343**	0.0827	1.2509	0.0825	1.2980	0.1014	1.3809	0.0901	1.2878	0.1004
120×30-5-2	Kruskal-Wallis	1.2558	0.1649	**1.2308**	0.0861	1.2877	0.1037	1.3459	0.1224	1.2519	0.1053
150×30-5-1	Kruskal-Wallis	**1.1717**	0.0724	1.1867	0.1168	1.2542	0.1872	1.2537	0.0952	1.1867	0.0576
150×30-5-2	ANOVA	**1.2338**	0.0717	1.2416	0.0772	1.2850	0.0921	1.3492	0.0928	1.2502	0.0833
80×20-5-1	ANOVA	**1.2635**	0.0888	1.3121	0.1113	1.3571	0.1115	1.4289	0.1055	1.3088	0.0798
80×20-5-2	Kruskal-Wallis	1.2899	0.1080	**1.2637**	0.0967	1.3554	0.1459	1.3836	0.0827	1.3006	0.1044

Table 8. Distance of the best trade-off solution to the ideal vector with baseline NSGAII and SPEA2.

Instance	MOEA/D T = 1%			MOEA/D T = 1.5%			MOEA/D T = 3%			NSGAII			SPEA2		
	δ_T	$\delta_{C_{max}}$	Δ	δ_T	$\delta_{C_{max}}$	Δ	δ_T	$\delta_{C_{max}}$	Δ	δ_T	$\delta_{C_{max}}$	Δ	δ_T	$\delta_{C_{max}}$	Δ
120×20-10-1	4.53%	1.51%	4.77%	4.68%	1.77%	5.01%	1.76%	1.06%	2.05%	**1.37%**	**0.74%**	**1.55%**	1.82%	0.89%	2.02%
120×20-10-2	3.45%	2.41%	4.21%	1.60%	2.28%	2.78%	1.46%	1.55%	2.13%	**0.74%**	**0.73%**	**1.04%**	1.77%	0.83%	1.96%
120×30-10-1	2.88%	1.56%	3.28%	3.20%	1.40%	3.49%	2.60%	**0.54%**	2.66%	2.53%	0.91%	2.69%	**1.68%**	0.58%	**1.78%**

Table 8. Continued.

120×30-10-2	6.74%	1.65%	6.94%	3.13%	1.45%	3.46%	**1.25%**	1.25%	**1.77%**	5.76%	0.75%	5.81%	3.37%	**0.70%**	3.44%
150×30-10-1	1.78%	2.25%	2.87%	4.27%	1.47%	4.52%	**1.27%**	0.77%	1.48%	1.67%	1.09%	2.00%	1.12%	**0.72%**	**1.33%**
150×30-10-2	3.83%	1.87%	4.26%	3.55%	0.83%	3.65%	**1.87%**	0.79%	**2.03%**	2.79%	0.61%	2.85%	2.55%	**0.53%**	2.60%
80×20-10-1	3.36%	1.34%	3.62%	2.74%	**0.72%**	2.83%	2.25%	0.76%	**2.38%**	**2.03%**	1.86%	2.75%	4.19%	1.08%	4.33%
80×20-10-2	5.52%	2.52%	6.07%	5.94%	1.83%	6.21%	**0.82%**	1.06%	**1.34%**	4.14%	1.65%	4.45%	2.59%	**0.98%**	2.78%
120×20-20-1	1.42%	2.57%	2.94%	3.51%	**0.64%**	3.57%	3.83%	1.14%	4.00%	**1.32%**	1.70%	**2.15%**	3.89%	1.53%	4.18%
120×20-20-2	**0.53%**	0.72%	**0.90%**	3.24%	0.77%	3.33%	1.46%	**0.28%**	1.49%	2.28%	0.45%	2.33%	2.41%	0.68%	2.51%
120×30-20-1	1.65%	2.58%	3.06%	3.42%	1.76%	3.84%	1.61%	1.74%	2.37%	3.56%	**0.73%**	3.63%	**1.17%**	1.56%	**1.95%**
120×30-20-2	3.60%	2.85%	4.59%	6.03%	2.00%	6.35%	3.79%	1.50%	4.08%	**3.01%**	1.66%	**3.44%**	3.80%	**1.11%**	3.96%
150×30-20-1	1.98%	1.75%	2.65%	1.65%	0.53%	1.73%	**0.15%**	**0.38%**	**0.41%**	1.98%	0.84%	2.15%	0.86%	0.92%	1.26%
150×30-20-2	4.01%	2.37%	4.66%	3.50%	1.22%	3.71%	**2.36%**	1.02%	**2.57%**	3.31%	1.34%	3.57%	3.96%	**0.40%**	3.99%
80×20-20-1	7.65%	3.18%	8.28%	6.28%	3.62%	7.25%	4.54%	3.00%	5.44%	**1.77%**	**2.82%**	**3.33%**	2.08%	**2.82%**	3.51%
80×20-20-2	4.41%	2.64%	5.14%	3.18%	1.69%	3.60%	**1.43%**	2.26%	**2.68%**	4.37%	1.95%	4.78%	3.45%	**1.13%**	3.63%
120×20-5-1	2.37%	1.95%	3.07%	1.78%	1.31%	2.21%	**1.46%**	1.10%	**1.82%**	2.00%	**0.55%**	2.07%	2.51%	1.31%	2.83%
120×20-5-2	3.37%	1.83%	3.84%	3.91%	1.38%	4.15%	**0.18%**	1.05%	**1.06%**	2.44%	**0.23%**	2.45%	2.06%	1.79%	2.73%
120×30-5-1	5.22%	1.15%	5.35%	3.98%	1.61%	4.29%	**1.92%**	**0.31%**	**1.94%**	3.32%	0.94%	3.45%	2.91%	0.88%	3.04%
120×30-5-2	4.63%	1.36%	4.83%	3.71%	1.36%	3.95%	2.07%	1.45%	2.53%	4.23%	**1.14%**	4.38%	**2.02%**	0.64%	**2.12%**
150×30-5-1	**1.86%**	1.23%	**2.23%**	2.49%	0.91%	2.65%	2.34%	**0.45%**	2.38%	2.68%	0.60%	2.75%	2.76%	1.02%	2.95%
150×30-5-2	3.44%	1.32%	3.68%	1.56%	1.16%	1.95%	**0.76%**	**0.44%**	**0.88%**	1.57%	0.76%	1.75%	2.57%	0.88%	2.72%
80×20-5-1	4.18%	2.38%	4.81%	3.37%	1.91%	3.88%	**1.99%**	2.08%	**2.88%**	3.20%	**0.70%**	3.28%	3.18%	1.23%	3.41%
80×20-5-2	4.31%	2.34%	4.90%	3.00%	1.78%	3.49%	3.59%	1.04%	3.74%	**2.16%**	**1.03%**	**2.39%**	3.07%	1.23%	3.31%
Average	3.61%	1.97%	4.21%	3.49%	1.48%	3.83%	1.95%	1.13%	2.34%	2.68%	1.07%	2.96%	2.58%	1.06%	2.85%

Figure 3 presents examples of the Pareto fronts computed for two representative instances solved in the experimental evaluation. In Figure 3-(a) the distance among the Pareto front is quite short while in Figure 3-(b), the Pareto front of the MOEA/D clearly outstrips the other MOEAs.

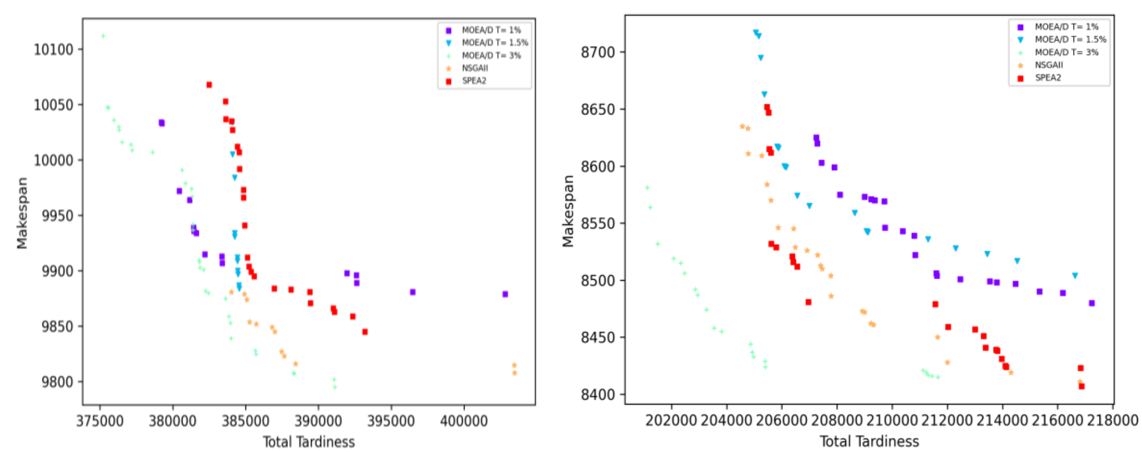

(a) Instance 150x30-5-1. (b) Instance 120x30-5-1.

Figure 4. Sample Pareto fronts computed by MOEA/Ds and baseline NSGAII and SPEA2 for representative instances.

4.4 Managerial Implications

Decision-making problems associated with production planning often incorporate different interests, so multi-objective approaches are appropriate to capture the full complexity of the process. In this case, the possibility of studying the impact that the fourth industrial revolution and personalized production will have, was explored. In this situation, the decision processes must adapt to this situation, and this is where the problem of missing operations gains preponderance. Given this situation, the results obtained in this work allow the identification of effective optimization methods to address the problem. In this particular case, a problem was addressed that seeks solutions to ensure a trade-off between the level of service provided to the client (seeking to minimize the delay in deliveries), and the use of productive resources (makespan).

In turn, it is interesting to note that the optimization approaches used in this case allow addressing problems where the production process is not static, since the different jobs have different numbers of operations. Therefore, the production environments addressed in this work are more general cases than those where all the jobs have the same set of operations (the latter is a particular case of the problem addressed here). A similar analysis could be extended to other variations between jobs, such as when jobs have different order arrival or release dates. These situations would imply considering problems of dynamic environments where the orders arrive on different dates. These types of problems, as well as the one studied here, allow us to contribute to generating efficient decisions, and facilitate the task of managers of productive operations.

5. Conclusions

Customized productions, driven by Industry 4.0 technologies, are generating new challenges for scheduling problems, as addressed in this case in a flow shop configuration. Among these new challenges, one of key importance is customer's order processing, since they are not all the same. Then, all jobs do not follow the complete route of operations of the flow shop, but rather some operations are not required. Even more, as it is a customer-oriented production system, the level of service provided must be considered within the planning of operations, which is why Total Tardiness was considered as an objective function. However, these market strategies must be provided within a framework of industrial efficiency, which allows obtaining the highest revenue from the production lines, which is why the makespan was also simultaneously considered as an objective function.

These missing operations and multi objective features add difficulty to an already NP-Hard problem. Thus, to achieve high quality solutions in reasonable times for industrial practice, an optimization approach based on metaheuristics was proposed in this work, particularly using MOEA/D.

This work proposed three variants of MOEA/D with different size for the neighborhoods for solving this combinatorial problem. Results show the validity of the proposed approaches. The RHV and spread multi objective optimization metrics were applied to analyze the results. Overall MOEA/D T =3% was able to obtain the best results of RHV, achieving accurate values (up to 0.9965). In terms of spread, MOEA/D T=1% was also able to obtain the accurate distributed solutions. The best trade-off solutions computed by the proposed MOEAs were compared with the ideal vector, showing a remarkable accuracy, with small deviations. In terms of the problem objectives, the MOEAs had small differences in makespan (1.03% on average for the MOEA/D T=3%). Additionally, the MOEA/D was compared with baseline NSGAII and SPEA2 which were previously developed for the same optimization problem. MOEA/D T=3% was able to obtain competitive results, being able to outperform NSGAII and SPEA2 in several instances. On the other hand, MOEA/D T=1% and T=1.5% show a good distribution of the solutions, outstripping NSGAII and SPEA2 in terms of spread in several instances.

Therefore, considering the results shown, MOEA/D approaches can be considered effective in addressing the problems of digitalized industries proposed by Industry 4.0. Moreover, these algorithms showed to be competitive when compared to other state-of-the-art metaheuristics.
As future lines of work, it would be interesting to propose some strategies that could take advantage of the decomposition structure of the MOEA/D, which allows a very good diversity in the population, but adding greater search depth. For this, the design and development of local search methods that favor convergence towards the Pareto front is proposed as a line of research. Likewise, another line of research could be to consider new objective functions that represent other interests of decision makers.

Conflict of Interest

The authors confirm that there is no conflict of interest to declare for this publication.

Acknowledgments

This research did not receive any specific grant from funding agencies in the public, commercial, or not-for-profit sectors. The experiments presented in this paper were carried out using ClusterUY (site: https://cluster.uy).

References

Alhindi, A., & Zhang, Q. (2014). MOEA/D with tabu search for multi objective permutation flow shop scheduling problems. In *2014 IEEE Congress on Evolutionary Computation (CEC)* (pp. 1155-1164). IEEE, USA.

Chang, P.C., Chen, S.H., Zhang, Q., & Lin, J.L. (2008, June). MOEA/D for flowshop scheduling problems. In *2008 IEEE Congress on Evolutionary Computation (IEEE World Congress on Computational Intelligence)* (pp. 1433-1438). IEEE, USA.

Coello, C., Lamont, G., & Veldhuizen, D. (2017). *Evolutionary algorithms for solving multi objective problems*. 2nd edition, Springer, New York.

Deb, K. (2001). Multiobjective optimization using evolutionary algorithms. John Wiley and Sons.

Dios, M., Fernandez-Viagas, V., & Framinan, J.M. (2018). Efficient heuristics for the hybrid flow shop scheduling problem with missing operations. *Computers & Industrial Engineering*, *115*, 88-99.

Glass, C.A., Gupta, J.N., & Potts, C.N. (1999). Two-machine no-wait flow shop scheduling with missing operations. *Mathematics of Operations Research*, *24*(4), 911-924.

Henneberg, M., & Neufeld, J. (2016). A constructive algorithm and a simulated annealing approach for solving flowshop problems with missing operations. *International Journal of Production Research*, *54*(12), 3534-3550.

Ishibuchi, H., & Nojima, Y. (2017). On the effect of normalization in MOEA/D for multi-objective and many-objective optimization. *Complex & Intelligent Systems*, *3*(4), 279-294.

Lee, J., Bagheri, B., & Kao, H.A. (2015). A cyber-physical systems architecture for industry 4.0-based manufacturing systems. *Manufacturing Letters*, *3*, 18-23.

Lenstra, J.K., Kan, A.R., & Brucker, P. (1977). Complexity of machine scheduling problems. In *Annals of Discrete Mathematics* (*Vol. 1*, pp. 343-362). Elsevier.

Marichelvam, M., & Prabaharan, T. (2014). Performance evaluation of an improved hybrid genetic scatter search (IHGSS) algorithm for multistage hybrid flow shop scheduling problems with missing operations. *International Journal of Industrial and Systems Engineering*, *16*(1), 120-141.

Minella, G., Ruiz, R., & Ciavotta, M. (2008). A review and evaluation of multiobjective algorithms for the flowshop scheduling problem. *INFORMS Journal on Computing*, *20*(3), 451-471.

Nesmachnow, S. (2014). An overview of metaheuristics: accurate and efficient methods for optimisation. *International Journal of Metaheuristics*, *3*(4), 320-347.

Nesmachnow, S., & Iturriaga, S. (2019). Cluster-UY: collaborative scientific high performance computing in Uruguay. In: *International Conference on Supercomputing in Mexico* (pp. 188-202). Springer, Cham.

Holthaus, O., & Rajendran, C. (2002). A study on the performance of scheduling rules in buffer-constrained dynamic flowshops. *International Journal of Production Research*, *40*(13), 3041-3052.

Pinedo, M.L. (2012). *Scheduling* (*Vol. 29*). New York: Springer.

Perez, A.T.E., Rossit, D.A., Tohme, F., & Vásquez, Ó.C. (2022). Mass customized/personalized manufacturing in Industry 4.0 and blockchain: Research challenges, main problems, and the design of an information architecture. *Information Fusion*, *79*, 44-57.

Pugazhendhi, S., Thiagarajan, S., Rajendran, C., & Anantharaman, N. (2003). Performance enhancement by using non-permutation schedules in flowline-based manufacturing systems. *Computers & Industrial Engineering*, *44*(1), 133-157.

Pugazhendhi, S., Thiagarajan, S., Rajendran, C., & Anantharaman, N. (2004a). Relative performance evaluation of permutation and non-permutation schedules in flowline-based manufacturing systems with flowtime objective. *The International Journal of Advanced Manufacturing Technology*, *23*(11-12), 820-830.

Pugazhendhi, S., Thiagarajan, S., Rajendran, C., & Anantharaman, N. (2004b). Generating non-permutation schedules in flowlinebased manufacturing sytems with sequence-dependent setup times of jobs: a heuristic approach. *The International Journal of Advanced Manufacturing Technology*, *23*(1-2), 64-78.

Rajendran, C., & Ziegler, H. (2001). A performance analysis of dispatching rules and a heuristic in static flowshops with missing operations of jobs. *European Journal of Operational Research*, *131*(3), 622-634.

Ramezanian, R., & Rahmani, D. (2017). MILP formulation and genetic algorithm for flow shop scheduling problem with missing operations. *International Journal of Operational Research*, *30*(3), 321-339.

Rossit, D.G., Toutouh, J., & Nesmachnow, S. (2020). Exact and heuristic approaches for multi-objective garbage accumulation points location in real scenarios. *Waste Management*, *105*, 467-481.

Rossit, D.A., Toncovich, A., Rossit, D.G., & Nesmachnow, S. (2021a). Solving a flow shop scheduling problem with missing operations in an Industry 4.0 production environment. *Journal of Project Management*, *6*(1), 33-44.

Rossit, D.A., Toncovich, A., Rossit, D.G., & Nesmachnow, S. (2021b). Flow Shop Scheduling Problems in Industry 4.0 Production Environments: Missing Operation Case. In *Handbook of Smart Materials, Technologies, and Devices: Applications of Industry 4.0* (pp. 1-23). Cham: Springer International Publishing.

Rossit, D.G., Rossit, D.A., & Nesmachnow, S. (2021c). Explicit multiobjective evolutionary algorithms for flow shop scheduling with missing operations. *Programming and Computer Software*, *47*(8), 615-630.

Rossit, D.G., Toncovich, A., & Fermani, M. (2021d). Routing in waste collection: A simulated annealing algorithm for an Argentinean case study. *Mathematical Biosciences and Engineering: MBE*, *18*(6), 9579-9605.

Shao, W., Shao, Z., & Pi, D. (2020). Modeling and multi-neighborhood iterated greedy algorithm for distributed hybrid flow shop scheduling problem. *Knowledge-Based Systems*, *194*, 105527.

Shao, W., Shao, Z., & Pi, D. (2021). Effective constructive heuristics for distributed no-wait flexible flow shop scheduling problem. *Computers & Operations Research*, *136*, 105482.

Toncovich, A., Rossit, D.A., Frutos, M., & Rossit, D.G. (2019). Solving a multi-objective manufacturing cell scheduling problem with the consideration of warehouses using a simulated annealing based procedure. *International Journal of Industrial Engineering Computations*, *10*(1), 1-16.

Toutouh, J., Rossit, D.G., & Nesmachnow, S. (2020). Soft computing methods for multiobjective location of garbage accumulation points in smart cities. *Annals of Mathematics and Artificial Intelligence*, *88*(1), 105-131.

Uniyal, N., Pant, S., & Kumar, A. (2020). An overview of few nature inspired optimization techniques and its reliability applications. *International Journal of Mathematical, Engineering and Management Sciences*, *5*(4), 732-743.

Venkataramanaiah, S. (2008). Scheduling in cellular manufacturing systems: an heuristic approach. *International Journal of Production Research*, *46*(2), 429-449.

Wang, Y., Ma, H.S., Yang, J.H., & Wang, K.S. (2017). Industry 4.0: a way from mass customization to mass personalization production. *Advances in Manufacturing*, *5*(4), 311-320.

Wang, G., Li, X., Gao, L., & Li, P. (2021). Energy-efficient distributed heterogeneous welding flow shop scheduling problem using a modified MOEA/D. *Swarm and Evolutionary Computation*, *62*, 100858.

Xu, L.D., Xu, E.L., & Li, L. (2018). Industry 4.0: state of the art and future trends. *International Journal of Production Research*, *56*(8), 2941-2962.

Yenisey, M.M., & Yagmahan, B. (2014). Multi-objective permutation flow shop scheduling problem: Literature review, classification and current trends. *Omega*, *45*, 119-135.

Zhang, Q., & Li, H. (2007). MOEA/D: A multiobjective evolutionary algorithm based on decomposition. *IEEE Transactions on Evolutionary Computation*, *11*(6), 712-731.